

Experimental studies on the utilization of steel slag in the steam-cured concrete

Han Fanghui¹ Liu Juanhong¹ He Xuejiang¹ Song Shaomin²

(¹School of Civil and Resource Engineering, University of Science and Technology Beijing, Beijing 100083, China)

(²School of Civil and Transportation Engineering, Beijing University of Civil Engineering and Architecture, Beijing 102616, China)

Abstract: The possibility of applying steel slag as mineral admixture in steam-cured concrete was investigated. The compressive strength, chloride permeability, carbonation depth and drying shrinkage of concrete and the microstructure characteristics of hardened paste were studied. Results show that the steam-cured concrete containing steel slag at a high water-to-binder ratio has low compressive strength, coarse pore structure, moderate permeability, large carbonation depth and great drying shrinkage. The negative effects of steel slag on the mechanical and durability performance of steam-cured concrete become smaller at a low water-to-binder ratio or by adding ultrafine ground granulated blast furnace slag (UGGBS). The later-age hydration of cement is significantly promoted by adding steel slag. The pozzolanic reaction and micro-filler effect of UGGBS result in dense structure, which makes great contribution to the strength development and durability performance of steam-cured concrete. These effects of steel slag and UGGBS are significant at a low water to binder ratio. The steam-cured concrete containing steel slag-UGGBS blended mineral admixture at a low water-to-binder ratio has the best performance with high compressive strength, fine pore structure and good durability.

Key words: steam curing; steel slag; compressive strength; hydration; durability

DOI: 10.3969/j.issn.1003-7985.2017.03.005

Precast concrete is commonly used in modern construction. The booming development of precast concrete can be explained by its many advantages^[1-2], such as assured quality control, a short construction period, simple fabrication process, etc. Steam curing is the most common method for the production of precast concrete. It accelerates the hydration of the binder by means of increasing temperature and humidity. The strength of concrete increases significantly. However, some researchers found that steam curing leads to poor performance of con-

crete at later ages^[3-5]. The coarse pore structure and heterogeneous distribution of hydration products reduce the strength and increase the permeability of concrete at later ages. Furthermore, the excessive increase in temperature causes the formation of delayed ettringite, which destroys the structure of concrete^[6]. Therefore, the maximum temperature of steam curing is usually lower than 70 °C^[2, 7].

In order to reduce the cost and decrease the emissions of carbon dioxide, mineral admixtures are widely used as partial replacement of Portland cement. The mineral admixture and Portland cement have different activities and different sensitivities to temperature^[8]. Therefore, the hydration of the composite binder is much more complicated under steam curing conditions. Cassagnabère et al.^[9] found that the strength of mortar containing 25% of metakaolin increases by 39% under the steam curing conditions after 1 d. It was due to the increasing amount of hydration products and the decreasing content of Ca(OH)₂ as well as the decrease in Ca/Si ratio. Ramezani-pour et al.^[10] reported that the steam curing clearly increased compressive strength by promoting hydration, and the highest compressive strength was obtained for the concrete containing metakaolin. Ho et al.^[11] found that a more porous structure was observed in the steam-cured concrete containing fly ash or slag. However, the addition of silica fume resulted in the best performance. Liu et al.^[12] noted that the demoulding compressive strength of the steam-cured concrete containing ultrafine fly ash was low. The ultrafine fly ash-slag blended mineral admixture increased the compressive strength of concrete.

According to the previous literature, the common mineral admixtures used in the steam-cured concrete are slag, fly ash and silica fume. However, the amount of these mineral admixtures is limited in China. In order to keep sustainable production of precast concrete and create a greener environment, more kinds of mineral admixtures should be developed. Steel slag is one of the important sources of industrial wastes, particularly in China^[13]. Steel slag consists of cementitious phases and non-active components. Owing to the low cooling rate, the reactivity of steel slag is lower than that of Portland cement. Mixing steel slag with ground granulated blast furnace slag at a proper ratio produces concrete with good performance^[14]. However, to the best of our knowledge, no

Received 2016-12-22.

Biography: Han Fanghui (1988—), female, doctor, lecturer, hanyang-1120@163.com.

Foundation items: Postdoctoral Science Foundation of China (No. 2015M580992, 2016T90036), the Open Fund of State Key Laboratory of High Performance Civil Engineering Materials (No. 2015CEM010).

Citation: Han Fanghui, Liu Juanhong, He Xuejiang, et al. Experimental studies on the utilization of steel slag in the steam-cured concrete[J]. Journal of Southeast University (English Edition), 2017, 33(3): 277 – 285. DOI: 10.3969/j.issn.1003-7985.2017.03.005.

research work has been carried out on the effects of steam curing on the hydration of the composite binder and the performance of concrete containing steel slag, particularly on the long-term strength development and the durability of the steam-cured concrete containing steel slag.

Therefore, in this paper, the compressive strength, chloride permeability, carbonation depth and drying shrinkage of the steam-cured concrete containing steel slag are investigated. Meanwhile, the non-evaporable water content and $\text{Ca}(\text{OH})_2$ content as well as the pore structure of the steam-cured paste containing steel slag are also studied. The purpose of this study is to investigate the utilization of steel slag in the steam-cured concrete.

1 Experiment

1.1 Raw materials

P. I 42.5 Portland cement, UGGBS and ground basic oxygen furnace steel slag from Tangshan, Hebei Province were used in this paper. The main mineral compositions of steel slag determined by XRD were C_2S , C_3S , C_2F and RO phase. The specific surface areas of Portland cement, UGGBS and steel slag were 362, 659 and 455 m^2/kg , respectively. The chemical compositions of raw materials are shown in Tab. 1.

Tab. 1 Mass fraction of chemical compositions of raw materials								%
Composition	CaO	MgO	SiO ₂	Al ₂ O ₃	Fe ₂ O ₃	MnO	SO ₃	LOI
Cement	60.25	3.26	21.13	4.55	2.43	3.51	2.56	1.93
Steel slag	38.19	6.87	20.29	5.24	22.37	3.68	0.57	2.31
UGGBS	39.47	8.68	30.14	18.64	0.75		0.24	1.04

The natural river sands with a maximum particle size of 5 mm and the fineness modulus of 2.7 were used as fine aggregates. The crushed limestones with the particle size of 5 to 25 mm were used as coarse aggregates.

initial slumps of the concretes were in the range of 180 to 200 mm. The NaOH solution with the pH value of 13.8 was prepared. Steel slag was mixed with NaOH solution to prepare the steel slag paste (SS). The NaOH solution to steel slag ratio was 0.4.

1.2 Test methods

The total content of steel slag and UGGBS is 40% in the steam-cured concrete. Tab. 2 and Tab. 3 show the mix proportions of pastes and concretes, respectively. The paste of 40 mm × 40 mm × 40 mm and concrete of 100 mm × 100 mm × 100 mm were prepared according to Tab. 2 and Tab. 3, respectively. 1% and 1.5% polycarboxylate superplasticizers were used for concretes with water-to-binder ratios of 0.4 and 0.3, respectively. The

Tab. 2 Mass fraction of mix proportions of pastes				
Sample	Water-to-binder ratio	Mix proportions/%		
		Cement	Steel slag	UGGBS
PC	0.4	100	0	0
PS1	0.4	70	30	0
PS2	0.3	70	30	0
PS3	0.4	60	30	10
PS4	0.3	60	30	10

Tab. 3 Mix proportions of concretes							kg/m ³
Sample	Cement	Steel slag	UGGBS	Fine aggregate	Coarse aggregate	Water	
C	450	0	0	751	1 038	180	
S1	315	135	0	751	1 038	180	
S2	315	135	0	771	1 064	135	
S3	270	135	45	751	1 038	180	
S4	270	135	45	771	1 064	135	

The total steam curing time was 24 h. The curing regimes of the steam-cured concrete are shown in Tab. 4.

Tab. 4 Curing regimes of the steam-cured concrete			
Pre-curing/h	Rate of temperature/(°C · h ⁻¹)	Maximum temperature/°C	Curing at maximum temperature/h
8	20	60	12

The samples were cured under the standard condition ((20 ± 1) °C, 95% RH) in the pre-curing period and after total steam curing. The compressive strengths of concretes were measured after curing for 1, 3, 28, 90 and 360 d.

acetone to terminate further hydration at the testing stage. The non-evaporable water content of the paste was determined by high temperature ignition and it was the mass difference between the hardened paste heated at 80 and 1 000 °C, and normalized by the mass after heating at 80 °C, finally corrected by the loss on ignition of raw materials^[15]. The $\text{Ca}(\text{OH})_2$ content of paste was measured by the thermogravimetric analyzer. It was carried out from 25 °C up to 900 °C at 10 °C/min and purged with nitrogen. The porosity, cumulative pore volume and pore size distribution of the paste were measured by a mercury intrusion porosimeter (MIP).

The chloride permeability of the steam-cured concrete after curing for 28, 90 and 360 d was determined accord-

ing to ASTM C1202 “Standard Test Method for Electrical Indication of Concrete’s Ability to Resist Chloride Ion Penetration”.

Concretes of 100 mm × 100 mm × 400 mm were prepared for the measurement of the carbonation depth of the steam-cured concrete. After total curing for 28 d, the concretes were placed in a room with a temperature of 20 °C and $(6 \pm 10)\%$ RH. The carbonation depth of concrete was determined after natural carbonating for 360 d. The visible interface between the carbonated and un-carbonated zone was observed by using one percent phenolphthalein in alcohol indicator solution. The carbonation depth was measured with the vernier caliper. The result of carbonation depth for one sample was the average value of thirty test points.

Concretes of 100 mm × 100 mm × 515 mm were prepared for the drying shrinkage test. The concretes were demoulded after total steam curing for 24 h. Then, the samples were cured under the standard condition for 2 d. After this, the concretes were installed onto the measuring device for drying shrinkage in an environment with (20 ± 1) °C and $(60 \pm 5)\%$ RH. The drying shrinkage of the steam-cured concrete was measured continuously for 360 d.

2 Results and Discussion

2.1 Compressive strength

In order to increase the production rate of precast concrete, the concrete needs to reach a certain compressive strength after initial steam curing. Thus, the moulds can be used for another casting. Fig. 1 gives the demoulding compressive strengths of concretes, which were cured for 1 d. The demoulding compressive strength of Sample S1 is clearly lower than that of Sample C. Although the initial steam curing accelerates the reaction of steel slag, the reaction rate of steel slag is still lower than that of cement due to its low activity. Furthermore, the early-age hydration rate of cement is decreased by adding steel slag^[13]. Thus, low demoulding compressive strength is obtained for Sample S1. Decreasing the water-to-binder ratio from 0.4 to 0.3 (Sample S2) or adding 10% of UGGBS (Sample S3) can increase the demoulding compressive strength. It is highlighted that the negative effect of steel slag on the demoulding compressive strength becomes smaller at a low water-to-binder ratio or by adding UGGBS. Owing to the high specific surface area and plenty of glass phases, the activity of UGGBS is higher than that of steel slag. The hydration of UGGBS is significantly promoted by steam curing. Meanwhile, the finer UGGBS particles fill the pores to densify the microstructure of the concrete. Therefore, the physical and chemical effects of UGGBS result in the steam-cured concrete with higher demoulding compressive strength. However, the demould-

ing compressive strengths of Samples S2 and S3 are still lower than Sample C. When decreasing the water-to-binder ratio of Sample S3 to 0.3, the demoulding compressive strength of Sample S4 is almost the same as that of Sample C; indicating that at low water-to-binder ratio, the concrete containing steel slag-UGGBS blended mineral admixture has high demoulding compressive strength after steam curing. The initial microstructure of concrete is dense due to the low water-to-binder ratio. The reaction of UGGBS produces additional C-S-H gel, which makes contribution to the strength of Sample S4.

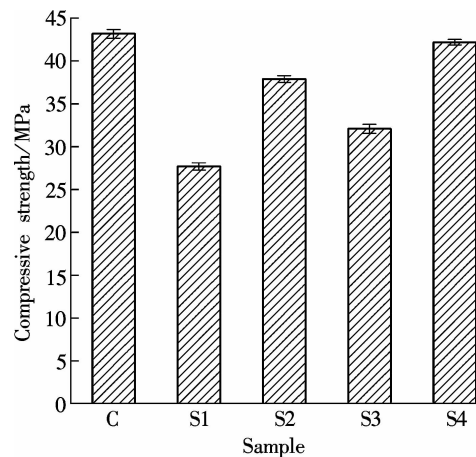


Fig. 1 Demoulding compressive strengths of concretes (cured for 1 d)

Fig. 2 presents the compressive strength development of the steam-cured concrete after demoulding. The compressive strength of Sample S1 is lower than that of Sample C at all testing stages. However, the gap between the compressive strength of Sample S2 and that of Sample C becomes smaller with prolonging ages. The compressive strength of Sample S2 is almost the same as that of Sample C at 90 d, and it is slightly higher than that of Sample C at 360 d. It indicates that decreasing the water-to-binder ratio can compensate for the negative effect of steel slag on the compressive strength at a high water-to-binder ratio. Increasing reaction of the steel slag makes contribu-

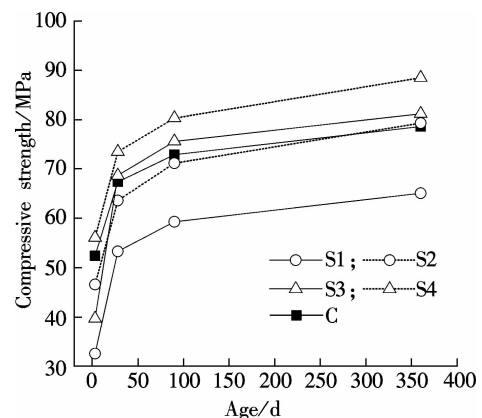


Fig. 2 Compressive strength development of steam-cured concrete after demoulding

tion to the later-age strength gain of concrete. Moreover, the later-age hydration of cement is promoted by adding steel slag^[15]. These contributions of steel slag are significant for the steam-cured concrete with low water-to-binder ratio, which has a dense structure with initial lower porosity. A small number of hydration products can further densify the structure. Thus, the high compressive strength of the concrete is obtained at later ages.

For the steam-cured concrete containing steel slag-UGGBS blended mineral admixture, the compressive strength of Sample S3 is still lower than that of Sample S2 at 3 d. But the strength growth rate of Sample S3 remains high from 3 to 28 d. The compressive strength of Sample S3 is higher than that of Sample C at later ages. The hydration of UGGBS is much more sensitive to temperature^[16]. Once the vitreous structure of UGGBS is destroyed by the elevated temperature, the reaction degree of UGGBS will increase along with prolonging age^[17]. UGGBS contributes greatly to strength development. Meanwhile, as mentioned above, the reaction of steel slag also increases the strength of the concrete at later ages. Note that the compressive strength of Sample S4 is higher than that of Sample C at all testing ages and the gap in strength between the two increases along with prolonging age. The pozzolanic reaction of UGGBS and the hydration of steel slag as well as the low water-to-binder ratio increase the strength of Sample S4. It is also highlighted that the steam-cured concrete with steel slag-UGGBS blended mineral admixture at a low water-to-binder ratio has a good long-term mechanical property.

2.2 Non-evaporable water content

The non-evaporable water content of the cement paste and paste containing steel slag are shown in Fig. 3. The non-evaporable water content of Sample PS1 is obviously lower than that of Sample PC at all studied ages. This indicates that a low content of hydrates is generated in Sample PS1. The findings are in accordance with the results of compressive strength (see Fig. 2). As expected, decreasing the water-to-binder ratio can decrease the non-evaporable water content. However, the ratios of the non-evaporable water content of Sample PS2 to that of Sample PS1 at 1, 3, 28, 90 and 360 d are 97.74%, 97.82%, 96.71%, 97.76% and 98.11%, respectively. The non-evaporable water content of paste containing 30% of steel slag is only decreased by 2% when decreasing the water-to-binder ratio from 0.4 to 0.3. In other words, the amount of hydration products is almost unchanged after decreasing the water-to-binder ratio. Meanwhile, the initial structure of paste is dense at a low water-to-binder ratio. Thus, the denser structure is obtained at later ages. Then, high compressive strength is achieved for Sample S2 (see Fig. 2).

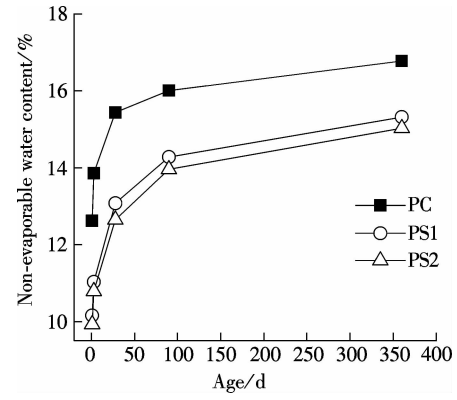


Fig. 3 Non-evaporable water content of cement paste and paste containing steel slag

Fig. 4 gives the non-evaporable water content of Sample PS1 and 70% PC + 30% SS. The 70% PC + 30% SS is defined by the sum of 70% of non-evaporable water content of Sample PC and 30% of non-evaporable water content of steel slag paste at the same curing age. It can be seen from Fig. 4 that the non-evaporable water content of 70% PC + 30% SS is lower than that of Sample PC at all studied ages and the gap between the two becomes larger at later ages. The hydration of Sample PS1 involves the fast hydration of cement and the slow reaction of steel slag. The 70% PC + 30% SS is basically regarded as the promoting effect of cement on the hydration of steel slag. Thus, the gap between the non-evaporable water content of Sample PS1 and that of 70% PC + 30% SS represents the promoting effect of steel slag on the hydration of cement. It is clear that steel slag has great promoting effect on the later-age hydration of cement. It is mainly due to the high water-to-cement ratio. Less water is consumed during the reaction of the steel slag. The adequate hydration of cement at later ages is beneficial to the strength gain of the steam-cured concrete (see Fig. 2). The promoting effect of steel slag on the later-age hydration of cement is greater at a low water-to-binder ratio due to the marginal effect. Thus, Sample S2 has higher compressive strength than Sample C at 360 d.

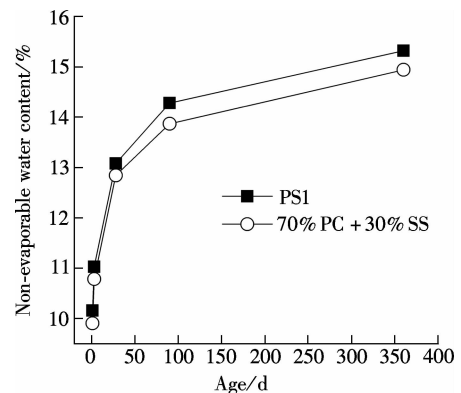


Fig. 4 Non-evaporable water contents of Sample PS1 and 70% PC + 30% SS

2.3 $\text{Ca}(\text{OH})_2$ content

The TG curves and $\text{Ca}(\text{OH})_2$ contents of Samples PS1 and PS3 at 360 d are given in Fig. 5. An obvious mass loss in the temperature range of about 400 to 500 °C, which represents the decomposition of $\text{Ca}(\text{OH})_2$, is observed in the TG curve (see Fig. 5(a)). The mass loss rate of Sample PS1 is higher than that of Sample PS3, indicating that the $\text{Ca}(\text{OH})_2$ content of Sample PS1 is higher than that of Sample PS3. The calculated $\text{Ca}(\text{OH})_2$ contents are 16.51% and 13.77% for Samples PS1 and PS3, respectively (see Fig. 5(b)). Sample PS3 has a low content of cement compared to Sample PS1. The reaction of UGGBS consumes a certain amount of $\text{Ca}(\text{OH})_2$. Thereby, a low content of $\text{Ca}(\text{OH})_2$ is determined. It is well known that $\text{Ca}(\text{OH})_2$ crystals have harmful effect on the microstructure and strength of concrete. The reaction of UGGBS consumes $\text{Ca}(\text{OH})_2$, which results in a low content of $\text{Ca}(\text{OH})_2$ and an additional amount of C-S-H gel. It is beneficial to the strength development. Therefore, the compressive strength of Sample S3 is much higher than that of Sample S1 (see Fig. 2). These effects of UGGBS are more significant in the concrete at a low water-to-binder ratio. The highest compressive strength is observed for Sample S4 (see Fig. 2).

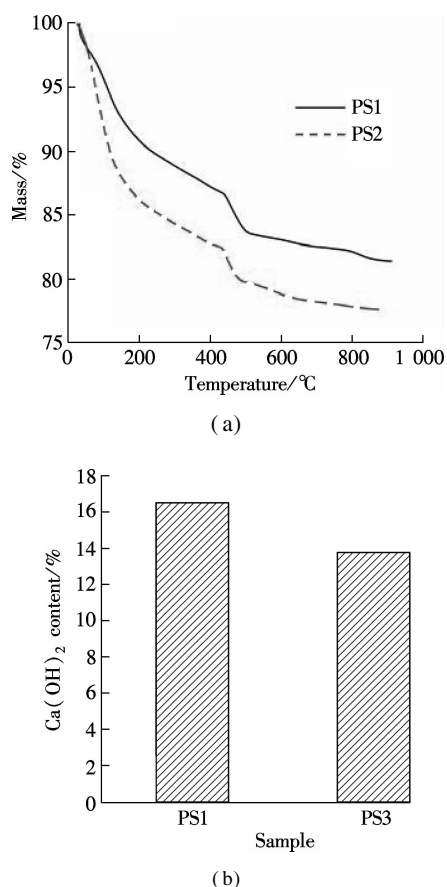


Fig. 5 TG curves and $\text{Ca}(\text{OH})_2$ contents of Samples PS1 and PS3 at the age of 360 d. (a) TG curves; (b) $\text{Ca}(\text{OH})_2$ contents

2.4 Pore structure

Fig. 6 shows the porosities of pastes cured for 28 and 360 d. An increase in curing age decreases the porosity for all samples. The porosity of Sample PS1 is obviously higher than that of Sample PC at 28 and 360 d. Low content of hydration products is generated for Sample PS1 at all studied ages (see Fig. 3). The limited amount of hydration products cannot fully fill the pores. The porosity of Sample PS2 is slightly higher than that of Sample PC at 28 d, and it is almost the same as that of Sample PC at 360 d. The negative effect of steel slag on the pore structure of paste is small at a low water-to-binder ratio. Sample PS3 has low porosity compared with Sample PS1, indicating that adding UGGBS also can refine the pore structure of the paste. Sample PS4 has the lowest porosity. This further confirms that steam-cured concrete containing steel slag-UGGBS blended mineral admixture at a low water-to-binder ratio has a dense structure. The findings are in line with the above analyzed results of compressive strength (see Fig. 2).

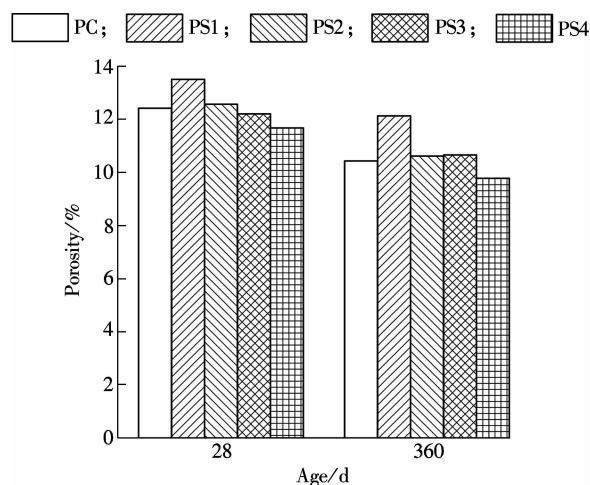


Fig. 6 Porosities of pastes cured for 28 and 360 d

Fig. 7 and Fig. 8 present the pore structures of hardened pastes cured for 28 and 360 d, respectively. It can be seen from Fig. 7 that the pore size related to the most probable pore diameter and the cumulative pore volume of Samples PS1 and PS2 are higher than that of Sample PC, particularly for Sample PS1. It is indicated that the pore structure of paste containing steel slag is coarser than that of Portland cement paste. At a high water-to-binder ratio, harmful pores (> 100 nm) are induced by adding steel slag (see Fig. 7(a)). For Sample PS2, although the porosity is slightly higher than that of Sample PC at 28 d (see Fig. 6), it merely increases the content of small pores (< 50 nm) (see Fig. 7(b)). The content of large pores (> 100 nm) significantly decreases, which is beneficial to the strength (see Fig. 2).

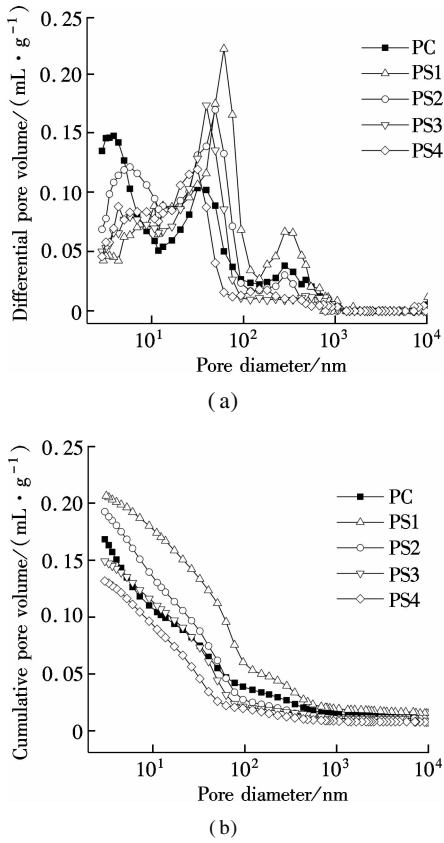


Fig. 7 Pore structure of hardened paste cured for 28 d.
(a) Pore size distributions; (b) Cumulative pore volume

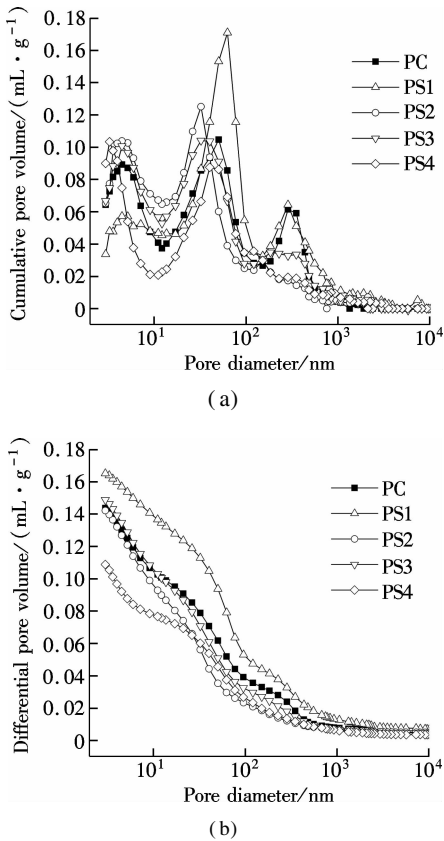


Fig. 8 Pore structure of hardened paste cured for 360 d.
(a) Pore size distributions; (b) Cumulative pore volume

The pore size related to the most probable pore diameter of Sample PS3 is almost the same as that of Sample PC (see Fig. 7(a)). The proportion of pores larger than 100 nm of Sample PS3 becomes smaller (see Fig. 7), revealing that the negative effect of steel slag on the pore structure can be compensated by incorporating UGGBS. The activity of UGGBS is stimulated by the initial steam curing. The pozzolanic reaction of UGGBS produces additional C-S-H gel, which entirely consists of crumpled foils^[18], refining the pore structure. Certainly, the micro-filler effect of UGGBS cannot be ignored. At a low water-to-binder ratio, the pore size related to the most probable pore diameter and the cumulative pore volume of Sample PS4 further decrease and a much denser structure is obtained for Sample PS4.

Fig. 8 shows that the pore structures of all samples are much finer at 360 d than those at 28 d. However, for Sample PS1, the pore size related to the most probable pore diameter and the cumulative pore volume are still larger than those of Sample PC. The findings are consistent with the results of compressive strength (see Fig. 2) and non-evaporable water content (see Fig. 3). An increase in age from 28 to 360 d significantly refines the pore structure of Sample PS2. It is due to the reaction of steel slag and the later-age promoting hydration of cement (see Fig. 4). The pore structures of Samples PS3 and PS4 are finer than that of Sample PC at 360 d. The dense structure with low porosity can be obtained for the steam-cured concrete containing steel slag-UGGBS blended mineral admixture at later ages, particularly at a low water-to-binder ratio.

2.5 Durability

2.5.1 Chloride permeability

The charge passed and permeability grade to chloride ion of the steam-cured concrete are shown in Fig. 9. As shown in Fig. 9(a), Samples C, S1, S2 and S3 exhibit moderate permeability at 28 d. It is attributed to the relatively high porosity of concrete. Owing to the low water-to-binder ratio and added UGGBS, Sample S4 presents a dense structure with low porosity (see Figs. 6 and 7(b)). Then low permeability is measured. At 90 d, Samples C and S3 exhibit low permeability. However, Samples S1 and S2 still exhibit moderate permeability. The compressive strength of Sample S2 is almost the same as that of Sample C at 90 d (see Fig. 2), but the permeability of Sample S2 is much higher (see Fig. 9(b)). It is probably because steel slag tends to enhance the connectivity of pores^[13]. Sample S4 exhibits very low permeability at 360 d. Samples C and S3 still exhibit low permeability, but the charge passed is much lower at 360 d than at 90 d. The charge passed of Sample S2 clearly decreases from 90 to 360 d, and thus low permeability is observed for Sample S2 at 360 d. However, Sample S1 still shows

moderate permeability at 360 d, indicating that the addition of steel slag can increase the permeability of steam-cured concrete at a high water-to-binder ratio. But at a low water-to-binder ratio, the steam-cured concrete containing steel slag shows low permeability at 360 d. The steel slag-UGGBS blended mineral admixture decreases the permeability of steam-cured concrete, particularly at the low water-to-binder ratio. The paste containing steel slag-UGGBS blended mineral admixture has fine pore structure (see Figs. 6 to 8). Meanwhile, the properties of interfacial transition zone can be improved by UGGBS acting as a micro-filler and consuming $\text{Ca}(\text{OH})_2$ (see Fig. 5). These effects are more significant for the steam-cured concrete at a low water-to-binder ratio. Thus, very low permeability is observed for Sample S4.

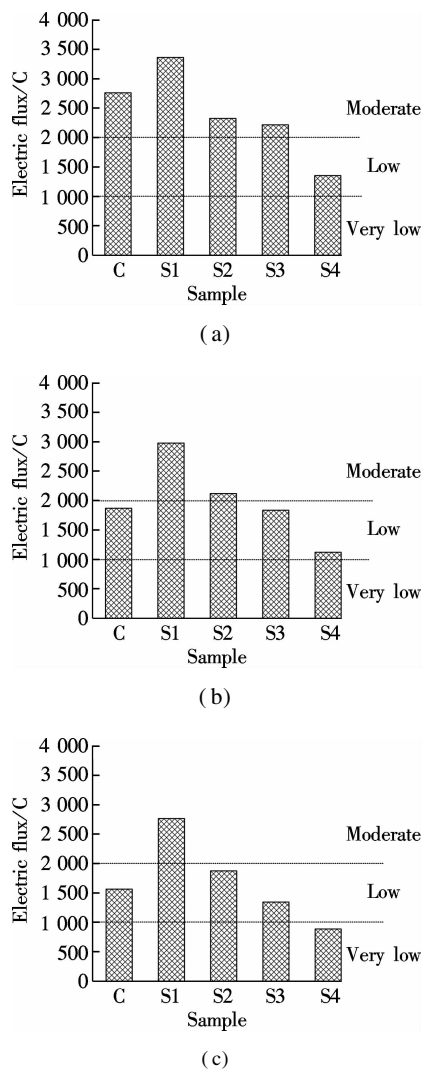


Fig. 9 Chloride permeability of steam-cured concrete. (a) 28 d; (b) 90 d and (c) 360 d

2.5.2 Carbonization depth

Fig. 10 presents the carbonization depth of the steam-cured concrete under natural conditions for 360 d. The carbonization depth of Sample S1 is much higher than that of Sample C. This is because the steam-cured concrete

containing steel slag at a high water-to-binder ratio has low compressive strength (see Fig. 2) and coarse pore structure (see Figs. 6 to 8) as well as high permeability (see Fig. 9). It is harmful to the carbonization resistance of concrete. The carbonization depths of Samples S2 and S3 are smaller than that of Sample S1. It is demonstrated that the steel slag has insignificant effect on the accelerating carbonation of steam-cured concrete at a low water-to-binder ratio or with the addition of UGGBS. The carbonation depths of Samples S2 and S3 are higher than that of Sample C, though their compressive strengths are higher than Sample C at 360 d (see Fig. 2). For Sample S2, the $\text{Ca}(\text{OH})_2$ content is low compared to Sample C. Furthermore, as explained above, steel slag tends to enhance the connectivity of pores. The charge passed of Sample S2 is high compared to Sample C at 360 d. Thus, a high carbonation depth is measured. For Sample S3, the content of $\text{Ca}(\text{OH})_2$ further decreases due to the low content of cement and the consumption of $\text{Ca}(\text{OH})_2$ during the pozzolanic reaction of UGGBS (see Fig. 5). Thus, the concrete tends to be carbonized. However, at a low water-to-binder ratio, although the $\text{Ca}(\text{OH})_2$ content is low in the steam-cured concrete containing steel slag-UGGBS blended mineral admixture, the structure is much denser with a fine pore structure (see Figs. 6 and 8) and very low permeability (see Fig. 9(c)). The carbonation depth of Sample S4 is only 0.7 mm at 360 d, which is much smaller than the carbonation depth of Sample C.

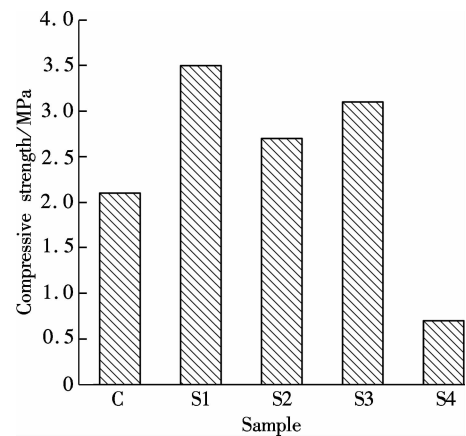


Fig. 10 Carbonation depth of steam-cured concrete under natural conditions for 360 d

2.5.3 Drying shrinkage

The drying shrinkages of all samples increase rapidly during 50 d (see Fig. 11(a)). The drying shrinkage of Sample S1 is slightly larger than that of Sample C. When samples are placed in a dry environment, the water loss of the steam-cured concrete containing a high content of steel slag at a high water-to-binder ratio is significant due to the slow hydration of the binder. The drying shrinkage of Sample S2 is almost the same as that of Sample S3 and their drying shrinkages are smaller than Sample C. The

steam-cured concrete containing steel slag-UGGBS blended mineral admixture at a low water-to-binder has the smallest value of drying shrinkage. As shown in Fig. 11 (b), the drying shrinkages are clearly distinguished among all the samples at later ages. The total drying shrinkage of Sample S1 during 360 d is evidently larger than that of Sample C. The values of total drying shrinkages of Samples C and S1 within 360 d are very close to each other. Small total drying shrinkages within 360 d are observed for Samples S3 and S4, particularly for Sample S4. It is demonstrated that the steel slag-UGGBS blended mineral admixture leads to the steam-cured concrete with a small drying shrinkage at a low water-to-binder ratio. The results are in agreement with the above analyzed results of chloride permeability (see Fig. 9(c)) and carbonation depth (see Fig. 10). From the above, the best performance is obtained from the steam-cured concrete containing steel slag-UGGBS blended mineral admixture at a low water-to-binder ratio.

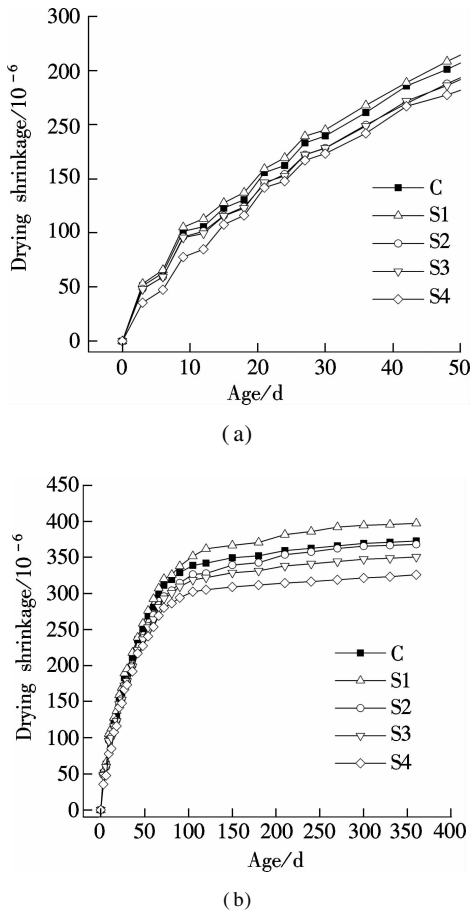


Fig. 11 Drying shrinkage of steam-cured concrete. (a) Initial 50 d; (b) Total testing ages

The steam-cured concrete containing steel slag has good performance if prepared with a low water-to-binder ratio. Moreover, mixing steel slag with highly active mineral admixture at a proper ratio also results in steam-cured concrete with better properties.

3 Conclusions

1) The demoulding compressive strength of steam-cured concrete with 30% steel slag at a high water-to-binder ratio is much lower than that of steam-cured cement concrete. Decreasing water to the binder ratio or adding UGGBS can increase the demoulding compressive strength, but their strengths are still lower than that of the steam-cured cement concrete. The demoulding compressive strength of the steam-cured concrete containing steel slag-UGGBS blended mineral admixture at a low water-to-binder ratio is almost the same as that of the steam-cured cement concrete.

2) The long-term compressive strength of steam-cured concrete with 30% steel slag at a high water-to-binder ratio is obviously lower than that of the steam-cured cement concrete. The low water-to-binder ratio or adding UGGBS is beneficial to the strength development of the steam-cured concrete. The steam-cured concrete containing steel slag-UGGBS blended mineral admixture at a low water-to-binder ratio has the highest compressive strength.

3) For paste containing 30% steel slag, the non-evaporable water content is much lower than that of cement paste at a high water-to-binder ratio, and decreasing the water-to-binder ratio from 0.4 to 0.3 almost does not change the amount of hydration products. Steel slag promotes the later-age hydration of cement. The $\text{Ca}(\text{OH})_2$ content of paste containing steel slag-UGGBS blended mineral admixture is lower than that of paste containing steel slag, which is beneficial to the strength.

4) At a high water-to-binder ratio, adding steel slag tends to make the pore structure coarser. But at a low water-to-binder ratio, the negative effect of the steel slag on the pore structure of the paste becomes smaller. The steel slag-UGGBS blended mineral admixture clearly refines the pore structure of the paste, particularly at a low water-to-binder ratio.

5) The steam-cured concrete containing steel slag at a high water-to-binder ratio exhibits moderate permeability and large carbonation depth as well as great drying shrinkage at all studied ages. Decreasing the water-to-binder ratio or adding UGGBS can reduce the negative effect of steel slag on the durability of steam-cured concrete. The best durability properties are obtained for the steam-cured concrete containing steel slag-UGGBS blended mineral admixture at a low water-to-binder ratio.

References

- [1] Maya L F, Zanuy C, Albajar L, et al. Experimental assessment of connections for precast concrete frames using ultra high performance fibre reinforced concrete [J]. *Construction and Building Materials*, 2013, **48**: 173 – 186. DOI: 10.1016/j.conbuildmat.2013.07.002.
- [2] Won I, Na Y, Kim J T, et al. Energy-efficient algorithms of the steam curing for the in situ production of

- precast concrete members [J]. *Energy and Buildings*, 2013, **64**: 275 – 284. DOI: 10.1016/j.enbuild.2013.05.019.
- [3] Han F H, Liu J H, Yan P Y. Effect of temperature on hydration of composite binder containing slag [J]. *Journal of the Chinese Ceramic Society*, 2016, **44**(8): 1071 – 1080.
- [4] Gallucci E, Zhang X, Scrivener K L. Effect of temperature on the microstructure of calcium silicate hydrate (C-S-H) [J]. *Cement and Concrete Research*, 2013, **53**: 185 – 195. DOI: 10.1016/j.cemconres.2013.06.008.
- [5] Lothenbach B, Winnefeld F, Alder C, et al. Effect of temperature on the pore solution, microstructure and hydration products of Portland cement pastes [J]. *Cement and Concrete Research*, 2007, **37**(4): 483 – 491. DOI: 10.1016/j.cemconres.2006.11.016.
- [6] Barbarulo R, Peycelon H, Prené S, et al. Delayed ettringite formation symptoms on mortars induced by high temperature due to cement heat of hydration or late thermal cycle [J]. *Cement and Concrete Research*, 2005, **35**(1): 125 – 131. DOI: 10.1016/j.cemconres.2004.05.041.
- [7] Ramezaniapour A A, Khazali M H, Vosoughi P. Effect of steam curing cycles on strength and durability of SCC: A case study in precast concrete [J]. *Construction and Building Materials*, 2013, **49**(6): 807 – 813. DOI: 10.1016/j.conbuildmat.2013.08.040.
- [8] Juenger M C G, Siddique R. Recent advances in understanding the role of supplementary cementitious materials in concrete [J]. *Cement and Concrete Research*, 2015, **78**: 71 – 80. DOI: 10.1016/j.cemconres.2015.03.018.
- [9] Cassagnabère F, Mouret M, Escadeillas G. Early hydration of clinker-slag-metakaolin combination in steam curing conditions, relation with mechanical properties [J]. *Cement and Concrete Research*, 2009, **39**(12): 1164 – 1173. DOI: 10.1016/j.cemconres.2009.07.023.
- [10] Ramezaniapour A M, Esmaeili Kh, Ghahari S A, et al. Influence of initial steam curing and different types of mineral additives on mechanical and durability properties of self-compacting concrete [J]. *Construction and Building Materials*, 2014, **73**: 187 – 194. DOI: 10.1016/j.conbuildmat.2014.09.072.
- [11] Ho D W S, Chua C W, Tam C T. Steam-cured concrete incorporating mineral admixtures [J]. *Cement and Concrete Research*, 2003, **33**(4): 595 – 601. DOI: 10.1016/S0008-8846(02)01028-1.
- [12] Liu B, Xie Y, Li J. Influence of steam curing on the compressive strength of concrete containing supplementary cementing materials [J]. *Cement and Concrete Research*, 2005, **35**(5): 994 – 998. DOI: 10.1016/j.cemconres.2004.05.044.
- [13] Wang Q, Yan P Y, Yang J W, et al. Influence of steel slag on mechanical properties and durability of concrete [J]. *Construction and Building Materials*, 2013, **47**(10): 1414 – 1420. DOI: 10.1016/j.conbuildmat.2013.06.044.
- [14] Wang Q, Yan P Y, Mi G D. Effect of blended steel slag-GBFS mineral admixture on hydration and strength of cement [J]. *Construction and Building Materials*, 2012, **35**(10): 8 – 14. DOI: 10.1016/j.conbuildmat.2012.02.085.
- [15] Han F H, Yan P Y. Hydration characteristics of slag-blended cement at different temperatures [J]. *Journal of Sustainable Cement-Based Materials*, 2015, **4**(1): 34 – 43. DOI: 10.1080/21650373.2014.959089.
- [16] Han F H, Liu R G, Wang D M, et al. Characteristics of the hydration heat evolution of composite binder at different hydrating temperature [J]. *Thermochimica Acta*, 2014, **586**(8): 52 – 57. DOI: 10.1016/j.tca.2014.04.010.
- [17] Yan P Y, Han, F H. Quantitative analysis of hydration degree of composite binder by image analysis and non-evaporable water content [J]. *Journal of the Chinese Ceramic Society*, 2015, **43**(10): 1331 – 1340.
- [18] Taylor R, Richardson I G, Brydson R M D. Composition and microstructure of 20-year-old ordinary Portland cement-ground granulated blast-furnace slag blends containing 0 to 100% slag [J]. *Cement and Concrete Research*, 2010, **40**(7): 971 – 983. DOI: 10.1016/j.cemconres.2010.02.012.

钢渣在蒸养混凝土中应用的实验研究

韩方晖¹ 刘娟红¹ 何薛江¹ 宋少民²

(¹ 北京科技大学土木与资源工程学院, 北京 100083)

(² 北京建筑大学土木与交通工程学院, 北京 102616)

摘要:旨在研究钢渣作为矿物掺合料在蒸养混凝土中应用的可能性. 研究了混凝土抗压强度、氯离子渗透性、碳化深度和干燥收缩及硬化浆体微结构特性. 结果表明:在高水胶比条件下,含钢渣蒸养混凝土的抗压强度低,孔结构粗化,渗透性等级为“中”,碳化深度和干燥收缩大. 降低水胶比或掺入超细矿渣可降低钢渣对蒸养混凝土力学性能和耐久性的负面影响. 掺加钢渣显著地促进了水泥的后期水化. 超细矿渣的火山灰反应和微集料填充效应使混凝土的结构致密,对混凝土的强度发展和耐久性有一定贡献. 在低水胶比条件下,钢渣和超细矿渣的作用更加明显. 低水胶比下含钢渣和超细矿渣复合矿物掺合料蒸养混凝土的性能最佳,获得的抗压强度高,孔结构细化,耐久性优异.

关键词:蒸养; 钢渣; 抗压强度; 水化; 耐久性

中图分类号: TQ172.11